ACS APPLIED MATERIALS & INTERFACES

Letter

www.acsami.org

# Simultaneously Harvesting Thermal and Mechanical Energies based on Flexible Hybrid Nanogenerator for Self-Powered Cathodic Protection

Hulin Zhang,*,† Shangjie Zhang,† Guang Yao,† Zhenlong Huang,† Yuhang Xie,† Yuanjie Su,† Weiqing Yang,‡ Chunhua Zheng,⊥ and Yuan Lin*,†

†State Key Laboratory of Electronic Thin Film and Integrated Devices, University of Electronic Science and Technology of China, Chengdu 610054, China

‡Key Laboratory of Advanced Technologies of Materials (Ministry of Education), School of Materials Science and Engineering, Southwest Jiaotong University, Chengdu 610031, China

⊥Department of Mathematics and Physics, Officers College of the Chinese People's Armed Police Forces, Chengdu 610213, China

*Supporting Information*

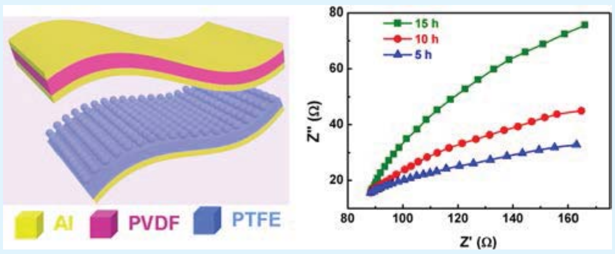


**ABSTRACT:** Metal corrosion occurs anytime and anywhere in nature and the corrosion prevention has a great significance everywhere in national economic development and daily life. Here, we demonstrate a flexible hybrid nanogenerator (NG) that is capable of simultaneously or individually harvesting ambient thermal and mechanical energies and used for a self-powered cathodic protection (CP) system without using an external power source. Because of its double peculiarities of both pyroelectric and piezoelectric properties, a polarized poly(vinylidene fluoride) (PVDF) film-based NG was constructed to scavenge both thermal and mechanical energies. As a supplementary, a triboelectric NG was constructed below the pyro/piezoelectric NG to grab ambient mechanical energy. The output power of the fabricated hybrid NG can be directly used to protect the metal surface from the chemical corrosion. Our results not only verify the feasibility of self-powered CP-based NGs, but also expand potential self-powered applications.

**KEYWORDS:** *hybrid nanogenerator, thermal energy, mechanical energy, self-powered, cathodic protection*

The thermal and mechanical energies are extremely abundant in our daily living environment. Harvesting ambient energy is becoming increasingly significant due to its critical significance for our long-term energy need and sustainable development.[1] In general, the thermal and mechanical energies can be scavenged based upon different physical effects. Thermal energy, aroused from the time-dependent temperature fluctuations, can be grabbed by utilizing pyroelectric NGs, which are based on pyroelectricity.[2−4] The piezoelectric effect is well-known as an effective approach to harvesting ambient mechanical energy.[5−7] Meanwhile, by coupling of triboelectrification and electrostatic induction, the triboelectric NG has been extensively demonstrated for converting various mechanical energies into electricity.[8−12] Because the thermal and mechanical energies are not always available at the same time in the actual environment, depending on day/night, working conditions, and some other cases, it is of significance and necessity to exploit a novel hybrid NG technology to simultaneously or individually harvest different energies by using a fully integrated energy cell.[13−15] As a result, small electronics can be powered by using whatever energy that is available at their working environment. Although some attempts about the integrated energy cells for harvesting two kinds of energies have been delivered,[16−19] there has been no report about a hybrid NG that consists of a pyroelectric NG, piezoelectric NG, and a triboelectric NG for simultaneously or individually harvesting thermal and mechanical energies. It is expected that this multimode energy harvesting device can be applied in a self-powered micro/nanosystem.

Seeking a novel and low-cost method to protect the metals from corrosion is greatly meaningful for the social and economic development. Various surface modification and treatment techniques for increasing the corrosion resistance of metals have been explored.[20−24] Nevertheless, CP is considered as a dominant way to protect the metals from corrosion.[25] Currently, there are three typical CP systems. The first type is the sacrificial anode CP system in which the metal electrode is electrically connected to a sacrificial anode.[26] More active metals are used to being sacrificed to protect the steels from corrosion. In this case, the protected area is limited related with the size of the sacrificed anode. The second one is the

**Received:** November 12, 2015
**Accepted:** December 16, 2015
**Published:** December 16, 2015

  

DOI: 10.1021/acsami.5b10923
*ACS Appl. Mater. Interfaces* 2015, 7, 28142−28147

impressed current CP system in which the metal is protected by applying cathodic current.[27] External power sources are essential for providing sufficient cathodic current, resulting in very high cost and environmental pollutions due to the periodical battery replacement. Photogenerated CP, as the last one, had been explored by coupling a semiconductor photoanode with a carbon steel electrode.[28] However, the appropriate ultraviolet light is indispensable. Hence, an ideal CP system is a self-powered system that can actively operate by easily and effectively grabbing ambient energy without employing external power sources.

In this paper, we have constructed a novel flexible hybrid NG, which can simultaneously or individually scavenge both ambient thermal and mechanical energies from the living environment. The hybrid NG has been demonstrated as an active power source instead of the external power source to achieve a self-powered CP system, which can effectively protect the metal from widely existed chemical corrosion.

## ■ EXPERIMENTAL DETAILS

**Preparation of the Nanostructure-Based PTFE Film.** To obtain a PTFE film modified with nanostructures, an inductively coupled plasma (ICP) reactive ion etching routine was utilized for etching PTFE film surface, which is very similar to that of the previous report.[9] The specific experimental procedure is illustrated in the Supporting Information.

**Fabrication of the Hybrid NG.** A polarized PVDF film with the thickness of 110 $\mu$m was selected to construct the pyroelectric and piezoelectric NGs. The PVDF film not only has the excellent pyroelectric and piezoelectric properties, but also can retain thermally, chemically and electronically stable at the temperature ranged from −40 to 80 °C. The PVDF film-based pyro/piezoelectric NG has the size of 3 cm × 2.5 cm, which is the same with that of the triboelectric NG at the bottom. The triboelectric NG can operate under the contact/separation between the PTFE film and the Al foil. A thermoelectric-based heater was employed to change the temperature of the hybrid device. The heater can stably and accurately control the temperature in the vicinity of the hybrid device. In addition, a thermometer was supplied to record the real-time temperature of the pyroelectric NG. The temperature changes and the mechanical vibration were applied on the hybrid device, respectively, when the pyroelectric, piezoelectric and triboelectric NGs were fully integrated. The performance (output voltage and current) of the hybrid NG device were collected by utilizing a low-noise voltage preamplifier and a current preamplifier (Stanford Research System model SR560 and SR570), respectively.

**Demonstration of the Self-Powered CP System.** The carbon steel electrodes with the exposed window area of 0.5 $cm^2$ were cleaned and polished by emery papers to remove the surface oxide layer, and then the obtained sheet were ultrasonically washed by acetone, isopropanol and deionized water, respectively. The simulated accelerated corrosion experiment was carried out in 0.1 M $NaNO_3$ electrolyte containing 0.1 M $NaHSO_3$, serving as ordinary rainwater. The simulated corrosion of the metal electrode coupled with and without the hybrid NG device (vibration frequency of 3 Hz and temperature variation period of 200 s) was conducted in a three-electrode electrochemical system using an electrochemical workstation (CHI 660E, Shanghai Chenhua Instrument Co., LTD, China). The rusted surface of the carbon steel electrode was characterized by using an optical microscope.

## ■ RESULTS AND DISCUSSION

The fabricated hybrid NG is sketched in Figure 1a. The materials selected here for the hybrid device construction are all flexible. The hybrid NG is composed of the top pyroelectric/piezoelectric NG and the bottom triboelectric NG. The top NG is based on the PVDF film with the top and bottom surface deposited with Al electrode layer. The thickness of the PVDF film and the coated Al electrode layer is about 110 $\mu$m and 10 nm, respectively. The triboelectric NG consists of the two Al layers and the PTFE film with the thickness of 200 $\mu$m. The upper Al layer plays dual roles as a triboelectric layer and as an electrode. The PTFE film serves as another triboelectric layer with the coated Al as the other electrode layer. In order to give rise to a more rough surface and a larger charge density, and therefore improve the triboelectrification between the layers,[9] a layer of nanostructures was created on the surface of the PTFE film via a typical dry-etching method using ICP, as described above. The average diameter of the nanostructures on the PTFE surface is less than 100 nm, as shown in Figure 1b. The real photograph of the fabricated hybrid device is also displayed in Figure S1, indicating a large flexibility of the hybrid NG device.

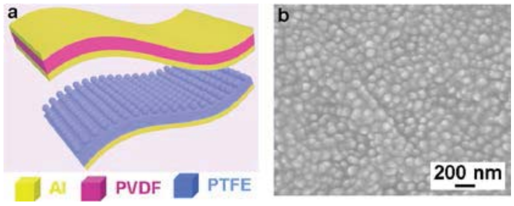


Figure 1. (a) Schematic diagram of the designed flexible hybrid NG. (b) SEM image of the PTFE surface modified with etched nanostructures.

To explore the performance of the hybrid NG, we first measured the output voltage/current of the PVDF film-based pyroelectric NG for harvesting thermal energy. The cyclic variation in temperature of the pyroelectric NG and the corresponding differential curve are displayed in Figure 2a. The positive and negative peak values of the temperature changing rate are about 3.8 and 5.7 K/s, respectively. A negative voltage/current pulse (3.2 V/0.1 $\mu$A) was observed when the temperature was increased from 293 to 313 K under the forward connection condition, as illustrated in Figure 2b. Conversely, there was a positive voltage/current pulse (3.6 V/0.12 $\mu$A) when the temperature was back to 293 K. The negative pulse is a little larger than that of the positive pulse, which can be attributed to the larger temperature changing rate. When the NG was reversely connected to the measurement instrument, the output voltage and current are plotted in Figure S2. The obtained opposite pulse signals indicate that the measured electric output signals were indeed generated by the fabricated device.

Meanwhile, we also demonstrated that the same PVDF-based device can be utilized to grab mechanical energy. Figure 2c shows the output voltage and current of the PVDF film-based piezoelectric NG under the forward connection to the measurement system. A positive voltage/current pulse (2.3 V/0.03 $\mu$A) was achieved when a compressive strain was applied on the device, as depicted in Figure 2c. Expectedly, after the release of the compressive strain, a negative voltage/current pulse was observed. By switching the polarity for electric connection with the measurement system, the piezoelectric output pulses with opposite sign were obtained, as plotted in Figure 2d. Obviously, the peaks of the piezoelectric output signals are much narrower than that of the pyroelectric output signals shown above.


DOI: 10.1021/acsami.5b10923
ACS Appl. Mater. Interfaces 2015, 7, 28142−28147

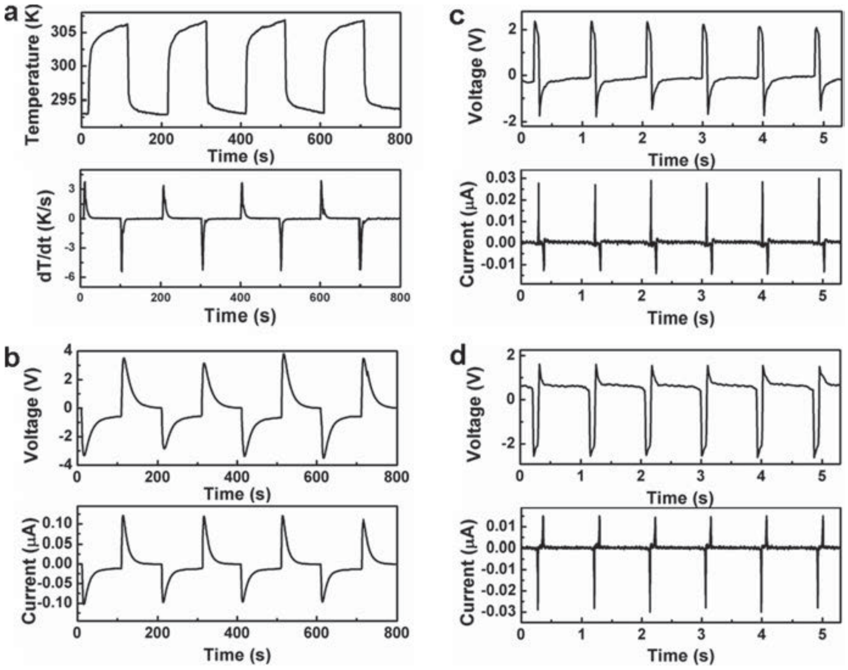

Figure 2. (a) Cyclic temperature change in the vicinity of the PVDF-based pyroelectric NG and the differential curve. (b) Corresponding output voltage and current of the pyroelectric NG under the forward connection with the measurement instrument. (c, d) Recorded output voltage and current of the PVDF-based piezoelectric NG applied with cyclic mechanical strain under the forward and reversed connection with the measurement system.

To verify the capability of the hybrid pyro/piezoelectric NG device for simultaneously and individually harvesting thermal and mechanical energies, Figure 3a exhibits the output voltage/current of the hybrid PVDF-based device. The output signals of the hybrid NG differ from that of two individual NGs, which is attributed to the heat-induced deformation of PVDF film. In general, the temperature of NG would raise as well as with a compressed strain created when the NG was touched by a hand. Figure 3b shows the hybrid pyroelectric and piezoelectric NG can be utilized to directly light up a LCD (with the display of "66"). The movie file presented in the Supporting Information indicates that the LCD can be lighted up when a hand touched the hybrid NG.

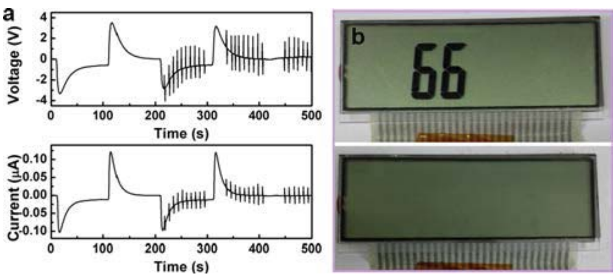

Figure 3. (a) Recorded output signals (voltage and current) of the hybrid pyroelectric and piezoelectric NGs. (b) Photographs of the lighted LCD powered by the electricity generated by the hybrid NG harvesting both thermal and mechanical energies, which was induced by hand touch. The bottom is the photograph of its original state.

To all sidedly harvest ambient mechanical energy, we integrated a triboelectric NG with the hybrid device, which can serve as an effective supplementary of the piezoelectric NG. Figure 4a, b illuminate the output performance of the fabricated triboelectric NG under the forward and reversed connection conditions, respectively. The output voltage can reach to 8 V with the current up to 0.42 $\mu$A. The operating principle of the triboelectric NG is based on the electron flow as driven by the triboelectrification coupled with electrostatic induction on the surfaces of the triboelectric layers (PTFE filmand Al foil).[8] The detailed operation mechanism is sketched in Figure S3. At the original state, a separation between the two plates remains at an angle on account of the polymer stiffness, as displayed in Figure S3a. When the externally compressive force induced by mechanical vibrations was applied, the PTFE film and the aluminum foil would get fully contacted. Because PTFE is much more triboelectrically negative than aluminum, electrons will be injected from aluminum into PTFE, as a result of generating positive triboelectric charges on the aluminum surface and negative charges on the PTFE surface.[8,9] All the triboelectric charges are balanced, then leading to no current in the external circuit (Figure S3b). Once the removal of compressive force occur during the mechanical vibration, the two triboelectric layers will separate with each other, resulting in an electric potential difference between the top Al layer and bottom Al electrode, which would drive electrons flow from the bottom Al electrode to the top Al layer through the external circuit (Figure S3c) to establish new electric equilibrium (Figure S 3d). It is known to all that the negative triboelectric charges can retain in a long time because of the intrinsic nature of the insulators. When the compressive force is conducted again, the electrons will flow back to bottom electrode (Figure S3e). Finally, two plates of the NG become in contact again (Figure S3b), which is a full cycle of the electricity generation. In practical terms, the compressive force and release induced by the external mechanical vibration are repeated again and again, leading to continuously generated electricity.


DOI: 10.1021/acsami.5b10923
ACS Appl. Mater. Interfaces 2015, 7, 28142−28147

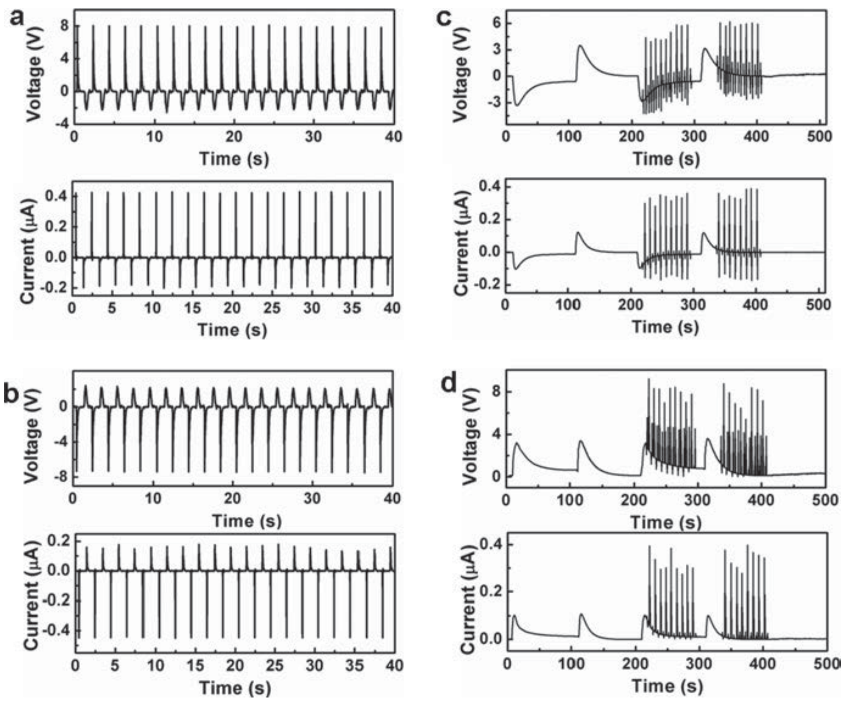


**Figure 4.** (a, b) Recorded output voltage and current of the PTFE-based triboelectric NG with cyclic contact and separation between two triboelectric layers induced by mechanical force under the forward and reversed connection conditions. (c) Output voltage and current of the hybrid pyroelectric, piezoelectric and triboelectric NGs. (d) Output signals of the hybrid NG with rectification by a full wave bridge circuit.

Figure 4c illustrates the output voltage and current of the hybrid device, indicating that the pyroelectric, piezoelectric and triboelectric NGs can effectively operate simultaneously and individually to grab thermal and mechanical energies from the ambient environment. Because of the alternative electric output signals of all the NGs, both the total output voltage and current sometimes declined rather than improved. To sufficiently use the harvested electricity, the output signals of the hybrid NG need to be rectified. The corresponding circuit schematic diagram of the measurement is illuminated in Figure S4. Figure 4d displays the output voltage and current of the hybrid NG after the output signals were rectified by a full wave bridge circuit. It can be obviously seen that all the NGs can operate simultaneously and individually to harvest ambient energies and the total output signals of the hybrid NG are always larger than that of the individuals.

To exploit the practical applications of the hybrid NG, we proved that the energies generated by the fabricated hybrid NG can be used for corrosion prevention. Figure 5 shows the schematic diagram of the self-powered electrochemical CP, indicating CP experiments of metal surface were connected with and without the CP of the hybrid NG. With respect to the CP system powered by the hybrid NG, the metal cathode was immersed into the electrolyte with a carbon rod served as the anode. The SEM image of the steel cathode before being submerged in electrolyte has been illustrated in Figure S5. The output signals of the hybrid NG were rectified, which was then connected to the electrochemical system. The recorded corrosion data were comparatively analyzed in the following section.

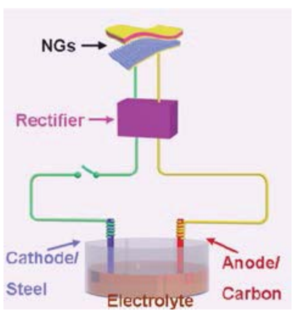


**Figure 5.** Schematic diagram of the self-powered CP system.

Rusts, as a typical corrosion product known to all, were usually chosen to intuitively indicate the corrosive state of a metal surface. The carbon steel specimens with and without CP were investigated by comparing their surface morphologies after simulated accelerated corrosion process. As comparatively illustrated in Figure 6a, for the specimens connected with CP

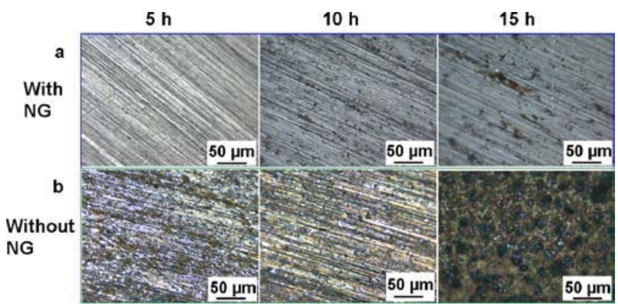


**Figure 6.** Micrographs of the surfaces of the carbon steel electrodes after the simulated accelerated corrosion (a) with and (b) without CP powered by the hybrid NG under the different durations (5, 10, and 15 h).



DOI: 10.1021/acsami.5b10923
*ACS Appl. Mater. Interfaces* 2015, 7, 28142−28147

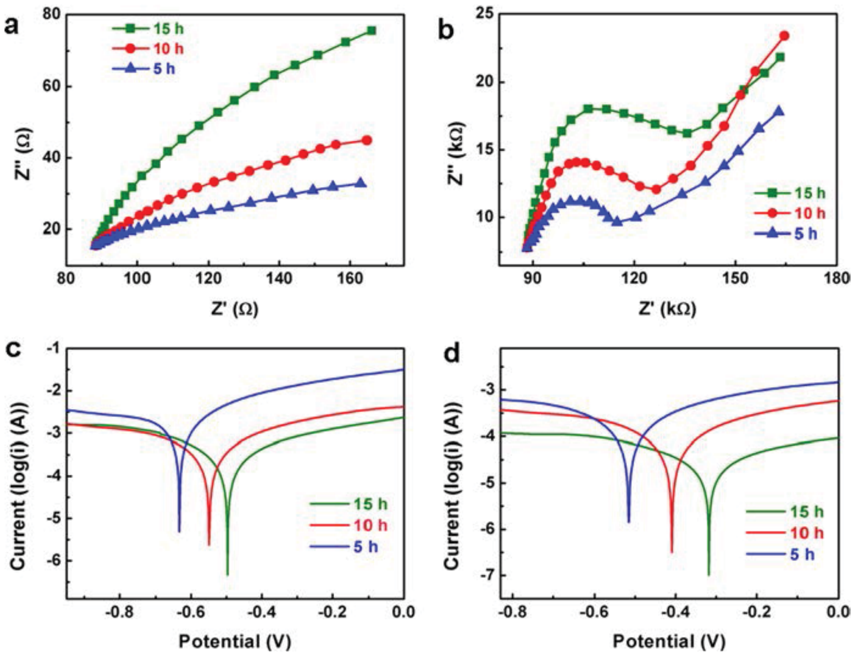


**Figure 7.** Nyquist diagrams of the carbon steel electrodes after the simulated accelerated corrosion (a) with and (b) without CP system powered by the hybrid NG under different durations (5, 10, and 15 h). The following Tafel polarization curves of the carbon steel electrodes after the simulated corrosion (c) with and (d) without CP system under different durations.

system powered by the hybrid NG, only a few gray spots presented on the surface without any apparent corrosion observed as corrosion time prolonged. However, pitting was yielded clearly in the Figure 6b, and more large pits were observed on the steel electrode which was corroded continuously in the simulated electrolyte for 15 h. In addition, the macro-morphological analysis of specimens is illustrated in Figure S6, exhibiting the same corrosive state. Both the micro and macro-morphological analysis confirm that the carbon steel electrodes can be effectively protected from corrosion with CP system powered by the hybrid NG device.

To further evaluate the corrosion protection, we performed electrochemical impedance spectroscopy (EIS) here. The typical Nyquist plots of the samples after simulated accelerated corrosion with and without the CP powered by the hybrid NG are depicted in Figure 7a, b, respectively. Evidently, the plots of the specimens connected with and without the CP systems indicate different electrochemical characteristics within the measuring frequency range. Figure 7a displays the impedance spectra measured on the specimens connected with CP systems. An obvious Faraday control process can be seen in Figure 7a, where radius of arches denotes the electron-transfer resistance of the electrochemical process.[30] The smaller radius of arches usually corresponds the less electrochemical reaction resistance, which, namely, means no or little rust layer formed on the steel electrode surface. It can be seen that, based on the radius of arches induced by the specimens, the reaction resistances of the electrodes are in the order of the one corroded for 5 h is less than that corroded for 10 h, which is less than that corroded for 15 h, which is in accord with the photographs presented in Figure 6 and Figure S6. For comparison, the EIS curves of the electrodes without CP are depicted in Figure 7b. All three impedance spectra indicate a slightly depressed capacitive arc in the high frequency region and a following linear trajectory at low frequencies, demonstrating the electrochemical reaction can be indexed to a Faraday and diffusion process, respectively.[29] The distorted arc at high frequencies is related to the electron-transfer resistance coupled with the double layer capacitance. It is known to all that the tailed linear diffusion is attributed to the Warburg impedance. Obviously, the electron-transfer resistance of the specimens with the CP system is much smaller than that without the CP and increases with the corrosion proceeding. The higher electron-transfer resistance corresponds to the broader rust layer. In other words, the rust film was produced on the surface of the specimens without the CP system.

Meanwhile, the quasi-steady-state polarization curves of all specimens were recorded after the simulated corrosion, which are presented in Figure 7c, d. It is found that all the polarization currents descended with the corrosion duration. However, the polarization potentials exhibit a positive shift, which is reversed to the polarization currents. More interesting is that the specimens connected with the CP powered by the hybrid NG have the lower polarization potentials than that without the CP during corrosion. The results further demonstrate the CP system powered by the hybrid NG device can indeed protect the specimen surface from corrosion, which agrees with the EIS data above.

In summary, we have successfully constructed the fully integrated flexible hybrid NG that is composed of a pyroelectric NG, a piezoelectric NG, and a triboelectric NG, which can be employed to simultaneously or individually harvest thermal and mechanical energies from the ambient environment. The top PVDF-based pyro/piezoelectric NGs can be utilized to power a LCD by grabbing both the thermal and mechanical energies induced by a hand touch. The bottom triboelectric NG was designed by coupling of triboelectrification and electrostatic induction between PTFE and Al layer to scavenge mechanical energy. The hybrid NG device was employed to fabricate a self-powered electrochemical corrosion prevention system. System-


DOI: 10.1021/acsami.5b10923
ACS Appl. Mater. Interfaces 2015, 7, 28142−28147

atic investigations were performed to demonstrate the effective CP powered by the hybrid NG. This work provides a novel approach to scavenging both ambient thermal and mechanical energies with low cost and high efficiency, using which a desirable self-powered CP system is established. This research has wide potential applications in energy conservation, environmental engineering, ocean engineering, and so on without supplying additional electric power.

## ■ ASSOCIATED CONTENT

### Ⓢ Supporting Information

The Supporting Information is available free of charge on the ACS Publications website at DOI: 10.1021/acsami.5b10923.

Real photograph of the fabricated hybrid device, the output voltage and current of the hybrid NG under the reversed connection condition, the circuit diagram of the self-powered CP driven by the hybrid NG, and the macro-morphological analysis of the steel electrodes (PDF)

Movie file including the hybrid NG for directly lighting up a LCD (AVI)

## ■ AUTHOR INFORMATION


### Corresponding Authors

*E-mail: zhangd198710@gmail.com.

*E-mail: linyuan@uestc.edu.cn.


### Notes

The authors declare no competing financial interest.

## ■ ACKNOWLEDGMENTS

This work was funded by the National Natural Science Foundation of China (No. 61504019), China Postdoctoral Science Foundation, and the National Basic Research Program of China (973 Program) under Grant No. 2015CB351905.

## ■ REFERENCES


(1) Dresselhaus, M. S.; Thomas, I. L. Alternative Energy Technologies. *Nature* **2001**, *414*, 332−337.

(2) Yang, Y.; Jung, J. H.; Yun, B. K.; Zhang, F.; Pradel, K. C.; Guo, W. X.; Wang, Z. L. Flexible Pyroelectric Nanogenerators using a Composite Structure of Lead-Free $KNbO_3$ Nanowires. *Adv. Mater.* **2012**, *24*, 5357−5362.

(3) Yang, Y.; Guo, W.; Pradel, K. C.; Zhu, G.; Zhou, Y.; Zhang, Y.; Hu, Y.; Lin, L.; Wang, Z. L. Pyroelectric Nanogenerators for Harvesting Thermoelectric Energy. *Nano Lett.* **2012**, *12*, 2833−2838.

(4) Yang, Y.; Wang, S.; Zhang, Y.; Wang, Z. L. Pyroelectric Nanogenerators for Driving Wireless Sensors. *Nano Lett.* **2012**, *12*, 6408−6413.

(5) Chang, C.; Tran, V. H.; Wang, J.; Fuh, Y.-K.; Lin, L. Direct-Write Piezoelectric Polymeric Nanogenerator with High Energy Conversion Effciency. *Nano Lett.* **2010**, *10*, 726−731.

(6) Chen, X.; Xu, S.; Yao, N.; Shi, Y. 1.6 V Nanogenerator for Mechanical Energy Harvesting Using PZT Nanofibers. *Nano Lett.* **2010**, *10*, 2133−2137.

(7) Wang, Z. L.; Song, J. Piezoelectric Nanogeneraors Based on Zinc Oxide Nanowires Arrays. *Science* **2006**, *312*, 242−246.

(8) Fan, F. R.; Tian, Z. Q.; Wang, Z. L. Flexible Triboelectric Generator. *Nano Energy* **2012**, *1*, 328−334.

(9) Wang, S. H.; Lin, L.; Wang, Z. L. Nanoscale Triboelectric-Effect-Enabled Energy Conversion for Sustainably Powering Portable Electronics. *Nano Lett.* **2012**, *12*, 6339−6346.

(10) Zhu, G.; Pan, C.; Guo, W.; Chen, C.; Zhou, Y.; Yu, R.; Wang, Z. L. Triboelectric-Generator-Driven Pulse Electrodeposition for Micro-patterning. *Nano Lett.* **2012**, *12*, 4960−4965.

(11) Zhang, H.; Yang, Y.; Su, Y.; Chen, J.; Adams, K.; Lee, S.; Hu, C.; Wang, Z. L. Triboelectric Nanogenerator for Harvesting Vibration Energy in Full Space and as Self-Powered Acceleration Sensor. *Adv. Funct. Mater.* **2014**, *24*, 1401−1407.

(12) Zhang, H.; Yang, Y.; Zhong, X.; Su, Y.; Zhou, Y.; Hu, C.; Wang, Z. L. Single-Electrode-Based Rotating Triboelectric Nanogenerator for Harvesting Energy from Tires. *ACS Nano* **2014**, *8*, 680−689.

(13) Xu, C.; Wang, X.; Wang, Z. L. Nanowire Structured Hybrid Cell for Concurrently Scavenging Solar and Mechanical Energies. *J. Am. Chem. Soc.* **2009**, *131*, 5866−5872.

(14) Xu, C.; Wang, Z. L. Compact Hybrid Cell Based on a Convoluted Nanowire Structure for Harvesting Solar and Mechanical Energy. *Adv. Mater.* **2011**, *23*, 873−877.

(15) Yang, Y.; Zhang, H. L.; Lin, Z.; Liu, Y.; Chen, J.; Lin, Z.; Zhou, Y.; Wong, C. P.; Wang, Z. L. A Hybrid Energy Cell for Self-Powered Water Splitting. *Energy Environ. Sci.* **2013**, *6*, 2429−2434.

(16) Hansen, B. J.; Liu, Y.; Yang, R.; Wang, Z. L. Hybrid Nanogenerator for Concurrently Harvesting Biomechanical and Biochemical Energy. *ACS Nano* **2010**, *4*, 3647−3652.

(17) Yang, Y.; Zhang, H. L.; Lee, S.; Kim, D.; Hwang, W.; Wang, Z. L. Hybrid Energy Cell for Degradation of Methyl Orange by Self-Powered Electrocatalytic Oxidation. *Nano Lett.* **2013**, *13*, 803−808.

(18) Pan, C.; Guo, W.; Dong, L.; Zhu, G.; Wang, Z. L. Optical Fiber-Based Core-Shell Coaxially Structured Hybrid Cells for Self-Powered Nanosystems. *Adv. Mater.* **2012**, *24*, 3356−3361.

(19) Pan, C.; Li, Z.; Guo, W.; Zhu, J.; Wang, Z. L. Fiber-Based Hybrid Nanogenerators for/as Self-Powered Systems in Biological Liquid. *Angew. Chem., Int. Ed.* **2011**, *50*, 11192−11196.

(20) Singh, R.; Dahotre, N. B. Corrosion Degradation and Prevention by Surface Modification of Biometallic Materials. *J. Mater. Sci.: Mater. Med.* **2007**, *18*, 725−751.

(21) Ye, C. Q.; Hu, R. G.; Dong, S. G.; Zhang, X. J.; Hou, R. Q.; Du, R. G.; Lin, C. J.; Pan, J. S. EIS Analysis on Chloride-Induced Corrosion Behavior of Reinforcement Steel in Simulated Carbonated Concrete Pore Solutions. *J. Electroanal. Chem.* **2013**, *688*, 275−281.

(22) Li, X.; Tao, J.; Guo, W.; Zhang, X.; Luo, J.; Chen, M.; Zhu, J.; Pan, C. A Self-Powered System Based on Triboelectric Nano-generators and Supercapacitors for Metal Corrosion Prevention. *J. Mater. Chem. A* **2015**, *3*, 22663−22668.

(23) Guo, W.; Li, X.; Chen, M.; Xu, L.; Dong, L.; Cao, X.; Tang, W.; Zhu, J.; Lin, C.; Pan, C. Electrochemical Cathodic Protection Powered by Triboelectric Nanogenerator. *Adv. Funct. Mater.* **2014**, *24*, 6691−6699.

(24) Zhu, H. R.; Tang, W.; Gao, C. Z.; Han, Y.; Li, T.; Cao, X.; Wang, Z. L. Self-Powered Metal Surface Anti-corrosion Protection Using Energy Harvested from Rain Drops and Wind. *Nano Energy* **2015**, *14*, 193−200.

(25) Cheung, M. M. S.; Cao, C. Application of Cathodic Protection for Controlling Macrocell Corrosion in Chloride Contaminated RC Structures. *Constr. Build. Mater.* **2013**, *45*, 199−207.

(26) Kim, J. G.; Joo, J. H.; Koo, S. J. Development of High-Driving Potential and High-Efficiency Mg-Based Sacrificial Anodes for Cathodic Protection. *J. Mater. Sci. Lett.* **2000**, *19*, 477−479.

(27) Xu, J.; Yao, W. Current Distribution in Reinforced Concrete Cathodic Protection System with Conductive Mortar Overlay Anode. *Constr. Build. Mater.* **2009**, *23*, 2220−2226.

(28) Yun, H.; Lin, C. J.; Li, J.; Wang, J. R.; Chen, H. B. Low-Temperature Hydrothermal Formation of a Net-like Structured $TiO_2$ Film and its Performance of Photogenerated Cathode Protection. *Appl. Surf. Sci.* **2008**, *255*, 2113−2117.

(29) Drazic, D. M.; Popic, J. P. Anomalous Dissolution of Metals and Chemical Corrosion. *J. Serb. Chem. Soc.* **2005**, *70*, 489−511.

(30) Mansfeld, F. Tafel Slopes and Corrosion Rates Obtained in the Pre-Tafel Region of Polarization Curves. *Corros. Sci.* **2005**, *47*, 3178−3186.